

Photograph Based Pair-matching Recognition of Human Faces

Min Yao, Kota Aoki, and Hiroshi Nagahashi

Abstract—In this paper, a novel system of pair-matching recognition of human faces without using face database between different color photographs is proposed. It mainly includes three parts: face detection, normalization and recognition. For face detection, a method of combination of Haar-like face detection, skin color segmentation and region-based histogram stretching and truncation (RHST) is proposed to achieve more accurate performance than only using Haar. Apart from an effective angle normalization method, side-face (pose) normalization, which is almost a fresh description but might be important and beneficial for the preprocessing work, is introduced. Then histogram-based and photometric illumination normalization methods are investigated and adaptive single scale retinex (ASR) is selected for its satisfactory illumination insensitivity. Finally, weighted multi-block local binary pattern (WLBP), together with 3 distance measures is applied for pair-matching recognition. Experimental results show its advantageous performance compared with PCA and multi-block LBP, based on a proposed evaluation principle.

Keywords—Face detection, pair-matching recognition, side-face normalization, skin color segmentation.

I. INTRODUCTION

THE key goal of the computer vision researchers is to develop a face detection and recognition system that can equal, and eventually surpass, human performance. Up to now, face detection and recognition has been attracting much attention, but we have rarely seen a complete recognition system weaving the former detection and the later recognition procedures, that can be deployed effectively in an unconstrained setting. Comprehensive surveys on the face detection are given in [1] and [2]. Face recognition can be searched in [3]. Usually stored databases of faces are used for recognition task.

In this paper, we propose a novel system of photograph based pair-matching recognition of human faces. This system recognizes (pair-matches) faces between several given color photographs with no database. Instead of deciding whether one face is contained in a stored database, we drive our research in a relatively different direction in which the recognition objects are all fresh faces from the photographs and no information of

the same faces stored previously come to help, which aims to simulate human ability to identify faces in a second glance with no previous impression. People have pair-matching ability and practice it often in their daily lives. For example, people may ask “do these photos both contain you” or “is that person who I just met” or start to talk to a person who is met the second time with this sentence “nice to meet you again”; it is also very popular on the internet that two face images of the same person with big contrast are displayed for comparison, one with make-ups and the other without make-ups, or one being the young face and the other the old face. Fig. 1 presents an example of detecting human faces between two different color photographs and a simple illustration for pair-matching recognition.

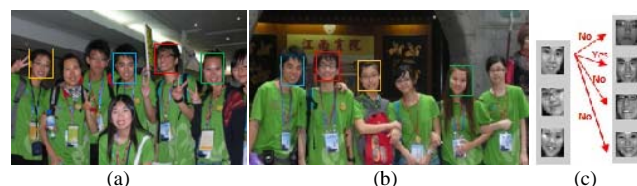


Fig. 1 (a) and (b) are two color photographs with manually detected rectangles, only four of which are drawn for illustration purpose and each pair with the same color indicates the same face. (c) shows two columns of faces corresponding to the two photos separately and gives one pair-matching illustration

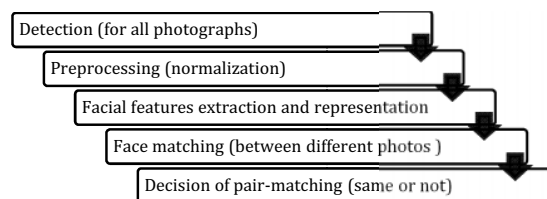


Fig. 2 Flowchart of our system.

Our recognition system contains five steps as shown in Fig. 2 and can be summarized by 3 main parts in order: face detection, normalization and recognition. The normalization step is necessary and important in our system since no database will provide referenced information of the same face images during the subsequent recognition step. Normalization adjusts the rough face images extracted by the detection step to be more standard and distinct. Then pair-matching recognition is manipulated based on extracted and normalized face images.

II. FACE DETECTION

For this step, we mainly employed Haar-like face detection method introduced and constructed by Viola and Jones [4]

Min Yao is now a doctor student of the Department of Information Processing, Tokyo Institute of Technology, R2-51, Yokohama 226-8503, Japan (phone: +81-(0)80-3910-8731; e-mail: yao.m.aa@m.titech.ac.jp).

Kota Aoki is with Imaging Science and Engineering Laboratory, Tokyo Institute of Technology, R2-51, Yokohama 226-8503, Japan (e-mail: aoki.k.af@m.titech.ac.jp).

Hiroshi Nagahashi is with Imaging Science and Engineering Laboratory, Tokyo Institute of Technology, R2-51, Yokohama 226-8503, Japan (e-mail: longb@isl.titech.ac.jp).

which is able to locate faces fast and guarantee the basic accuracy. But before it we used Histogram Stretching and Truncation (HST) to remove the extreme illumination of the original photos. In this way, the intensity of some specific regions of the photos would not be too light or too dark; the contrast of the photos is enhanced and facial features are highlighted. Also Haar-like face detection may find non-facial features by mistake and therefore skin color segmentation was used to extract the skin region candidates that are likely to represent faces. By the combination of these three operations, the false detection and missed detection can be tackled.

A. Haar-like Face Detection

Haar-like face detector contains three main ideas that make it possible to build a successful face detector that can run in real time: the integral image, classifier learning with AdaBoost, and the cascade structure.

In our system, rectangular Haar-like features are used due to its key advantage of fast calculation speed. It considers adjacent rectangular regions at a specific location in a detection window, sums up the pixel intensities in these regions and calculates the difference between them, in which way, the existence of oriented contrasts between regions in the image such as edges or changes in texture are encoded. There are 3 kinds of rectangular Haar-like features as shown in Fig. 3 (a). Fig. 3 (b) displays some rectangular Haar-like features of true faces.

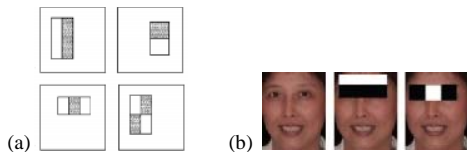


Fig. 3 (a) Examples of rectangular features shown relative to the enclosing detection window. (b): Examples of vertical two-rectangular Haar-like feature and horizontal three-rectangular Haar-like feature of true faces.

Then integral image is chosen to yield fast feature computation. It is based on summed area table [5] and can be defined as two-dimensional lookup tables in the form of a matrix with the same size of the original image. Each element of the integral image at location x, y contains the sum of all pixels located on the up-left region of x, y , inclusive:

$$ii(x, y) = \sum_{x' \leq x, y' \leq y} i(x', y') \quad (1)$$

where $ii(x, y)$ is the integral image and $i(x, y)$ is the original image (see Fig. 4 (a)). The integral image can be computed in one pass over the original image. Using the integral image any rectangular sum can be computed in only four array references (lookups) (see Fig. 4 (b)).

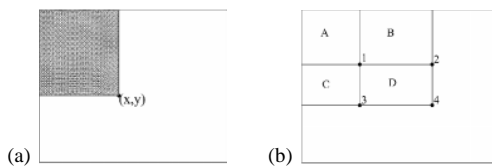


Fig. 4 (a) The value of the integral image at point (x, y) is the sum of all the pixels above and to the left. (b): The sum of the pixels within rectangle D can be computed with four array references.

The whole system is developed by constructing a cascade of classifiers. Stages in the cascade are created by training classifiers using AdaBoost, a learning algorithm that combines a collection of weak learners to form a stronger classifier. AdaBoost restricts the weak learner to the set of classification functions each of which depends on a single feature and the weak learning algorithm is designed to select the single rectangular feature which best separates the positive and negative examples. For each feature, the weak learner determines the optimal threshold classification function, such that the minimum number of examples is misclassified. A weak classifier $(h(x, f, p, \theta))$ thus consists of a feature (f), a threshold (θ) and a polarity (p) indicating the direction of the inequality:

$$h(x, f, p, \theta) = \begin{cases} 1 & \text{if } pf(x) < p\theta \\ 0 & \text{otherwise} \end{cases} \quad (2)$$

where x is a 24×24 pixel sub-window of an image. Each successive classifier is trained only on those selected samples which pass through the preceding classifiers. If at any stage in the cascade a classifier rejects the sub-window under inspection, no further processing is performed but continue on searching the next sub-window (see Fig. 5). Starting with a two-feature strong classifier, an effective face filter can be obtained by adjusting the strong classifier threshold to minimize false negatives. The initial AdaBoost threshold is designed to yield a low error rate on the training data. A lower threshold yields higher detection rate.

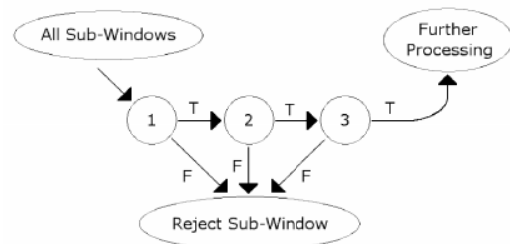


Fig. 5 The face detection cascade [7]

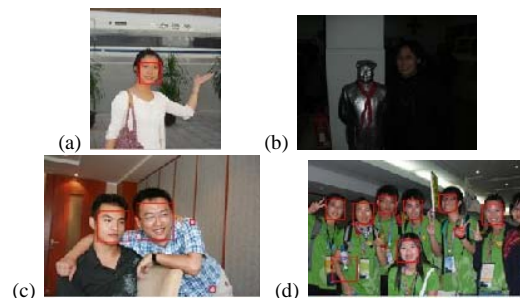


Fig. 6 Examples of face detection using Haar-like features. (a): Result of correct detection; (b): result with missing detection; (c) and (d): result with false detections

B. Skin Color Segmentation

Haar-like face detection is likely to cause false detection due to the usage of oriented gradients description which is too delicate pattern to focus only on facial features. Face skin region is a relatively integral and broad part notable from the background in most natural situations. So we used skin color segmentation as an auxiliary implementation to enclose the face

detection within human parts.

Different skin colors are tightly clustered. According to many previous skin color analysis works [8, 9], in order to omit the influence of luminance, we choose $YCbCr$ and HSV color spaces to do pixel-based skin detection and then apply few pixel connected components removing method and dilation to get rid of noise points and emphasize the skin regions. Here we set the ranges of components C_b , C_r and H as [77,140], [133,173] and $[0,0.1] \cup [0.9,1]$ separately. Fig. 7 are examples of skin color segmentation and Fig. 8 shows several comparison results.



Fig. 7 (a1), (b1) are original photographs; (a2), (b2) are skin detection results; (a3), (b3) are final skin segmentation results

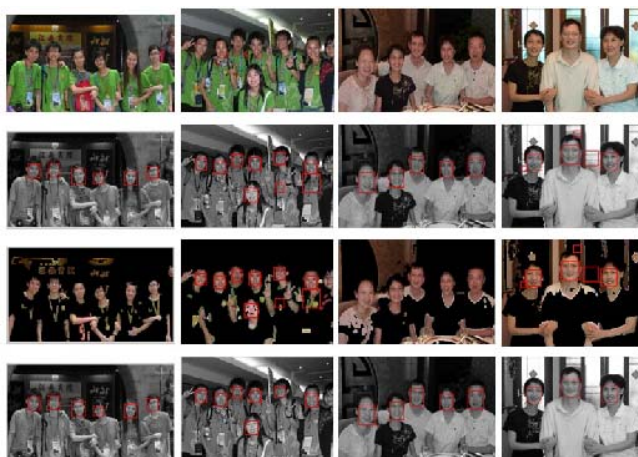


Fig. 8 The first row are original photographs; the second are Haar-like face detection results; the third are skin color segmentation results; the final row are results combining the Haar-like detection and skin color segmentation

C. Illumination Consideration

As Fig. 6 tells us, when extreme illumination problem comes to interfere, detection performance will badly fall down leading to serious missed detection. So we further consider about using Histogram Stretching and Truncation (HST) to eliminate severe illumination. But sometimes the detection suffers from locally uneven illumination rather than the overall extreme illumination, so HST has to be operated within specific regions. We call this region-based HST as RHST. Two examples using HST are shown in Fig. 9 and the corresponding Haar-like detection results are shown in Fig. 10.

Now we just applied the manual region selection for HST

and it may be misunderstood that the region should be faces. In fact, the selected regions only need to be parts which are too dark or light on average in case that there are faces within these regions. We further consider about automatic region selection and segmentation. Otsu [10] is one of the possible methods. Otsu can automatically segment one photograph into several parts within which the pixels are of the similar intensity range and the number of the parts is according to the extent to which the photo is uneven. Actually more parts are better so that we can divide extremely illuminated parts more precisely and these parts would be the selected regions for HST. Fig. 11 shows an example using Otsu to do the two parts segmentation and the relatively dark region is set as black. If we do the HST within the dark region, we may emphasize the face features within it and assist the Haar method to extract the missed faces.



Fig. 9 Illumination removal by HST over photographs under overall extreme illumination and locally uneven illumination



Fig. 10 Results of Haar-like detection without and with (R)HST



Fig. 11 Two parts segmentation using Otsu method

D. Combination

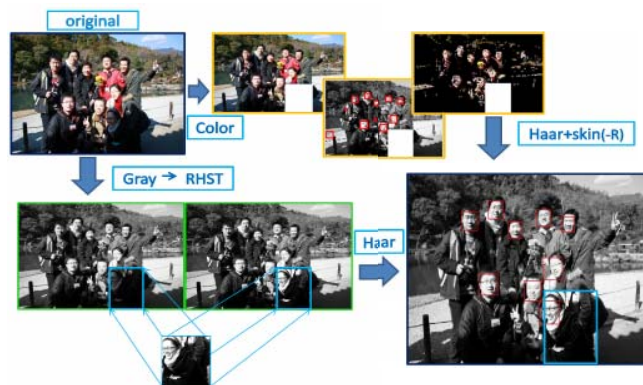


Fig. 12 Scheme of our proposed method—RHST+Skin(-R) (combination of Haar-like face detection, skin segmentation and RHST)

Haar-like face detection is fast and efficient in most detection task but false detection and missed detection exist. Skin color gives useful information and skin color segmentation can serve as a kind of sweeper helping Haar method get rid of fragile false detection. Illumination problems cause missed detection, so the HST illumination normalization method is brought about. Although the general HST is fit for dealing with the overall extreme illumination problem, uneven illumination is tackled by region-based HST (RHST). Here we present the final scheme of face detection which is the combination of Haar-like face detection, skin color segmentation and RHST, as shown in Fig. 12. The skin color segmentation is applied to the parts without the selected regions for HST; the Haar-like method is operated with the skin segmentation to try to avoid false detection; the combination of Haar-like method and RHST reduces missed detection.

III. FACE NORMALIZATION

The goal of this step is to obtain upright, frontal, normally lighted and distinct faces. Here we focus on the geometric (angle, size, pose) and illumination normalization.

A. Geometric Normalization

We firstly apply Hough circle detection to locate eyes since the position of eyes reflects the situation of a face. Sample results of eye location are given in Fig. 13. By using the position of eyes, the angle of a face can be successfully measured. Then with the angle, we use 2D basic rotation transformation [11] to rotate the face about the pivot point of the face image. The matrix form of 2D basic rotation transformation (for anticlockwise direction) is shown as (3). For each face point, if the rotated position (x', y') is integer the position is directly calculated and otherwise bilinear interpolation is applied to gain the rotated position. Fig. 14 shows several angle normalization results.

$$\begin{bmatrix} x' \\ y' \\ 1 \end{bmatrix} = \begin{bmatrix} \cos \theta & -\sin \theta & 0 \\ \sin \theta & \cos \theta & 0 \\ 0 & 0 & 1 \end{bmatrix} \begin{bmatrix} x \\ y \\ 1 \end{bmatrix} \quad (3)$$



Fig. 13 (a) eyes location using Hough circle detection; (b): illustration of face angle measurement



Fig. 14 Extracted face images and angle normalized ones.



Fig. 15 Size normalized face images

All the extracted face images after angle normalization are cropped to the size of 112x92 as illustrated by Fig. 15. This is partly due to the later recognition step using the PCA algorithm which trains out a set of eigenvectors based on the ORL database created by AT&T Laboratories Cambridge and face images from this database are uniformly set to size of 112x92.

In our research, we also generate a novel idea about the 3D pose normalization and we call it side-face normalization. Actually face pose is one main aspect that torture faces of the natural photographs from the standard view and significantly impact on the recognition effect. Common sense reminds us that 3D models of faces may be advantageous in doing the pose normalization yet consuming much time and inaccessible information. For the side-face normalization, we first need to make sure that the turning of the face is not too deep. This prerequisite is measured by calculating the turning rate of the face based on the nose location and face region demarcation and Fig. 16 gives the procedure to measure face turning rate.

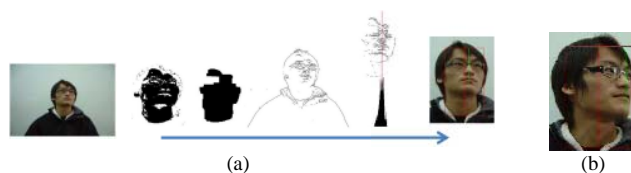


Fig. 16 (a) procedure for nose location and face region demarcation; (b): sample face image with too deep face turning

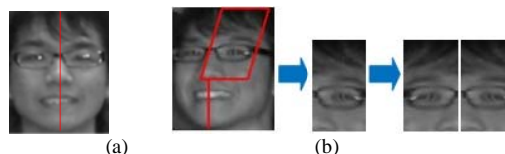


Fig. 17 Illustration of the frontal face images and how the side-face is segmented and normalized into frontal face

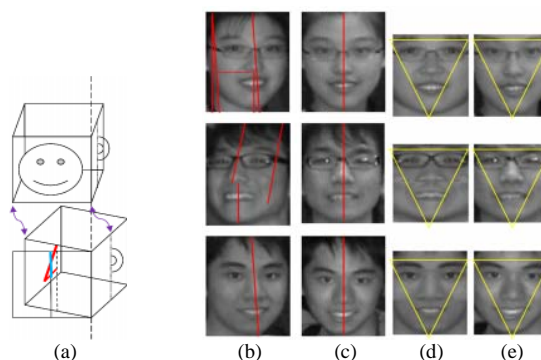


Fig. 18 (a) Illustration of the corresponding relationship between side face and frontal face; (b): comparison between side-face normalized face images and frontal face images

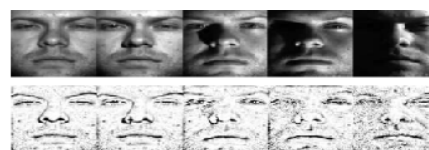


Fig. 19 The first row are face images from Cropped Yale Face Database B [14] and the second are the corresponding ASR face images



Fig. 20 Two groups of original extracted face images from two photographs (1st row), geometrically normalized face images (2nd row) and ASR face images (3rd row)

Then we simply apply the idea that human faces are symmetric and by twisting integral half of the face, a frontal half of the face can be obtained. The half part can be represented by the red diamond shape region illustrated in Fig. 17. By connecting this half and its horizontal overturn, with the mouth gained in the same way, we can get the final rough frontal face. Fig. 18 (d) shows some final side-face normalization results. Compared with Fig. 18 (e) of normal frontal faces, we can see that the features of faces can be maintained to a large extent.

B. Illumination Normalization

For the illumination normalization in our research 6 histogram based methods and 12 photometric methods are compared and a toolbox named INface (Illumination Normalization techniques for robust Face recognition) created by [12] is applied to achieve the testing job. The method of Adaptive Single Scale Retinex (ASR) [13] was selected in our system. It estimates the illumination by iteratively convolving the original input image with 3×3 mask weighted by a coefficient combining two measures of the illumination discontinuity at each pixel. See Fig. 19 and Fig. 20 for sample results.

IV. FACE RECOGNITION

This part is a challenging job because the facial features of a person can only be extracted from the current face images. Even though the previous normalization step has reduced variant environmental influences, we have to apply robust and distinguishing recognition method. Here lists several famous recognition algorithms divided into two categories:

- Feature-based: Elastic Bunch Graph Matching (EBGM), template, etc.
- Holistic:
 - Statistical: PCA, ICA, LDA, kernel methods, AAM, LBP, etc.
 - AI (artificial intelligence): SVM, HMM, etc.

In our system, the method of weighted multi-block local binary pattern (WLBP) [17] is used for pair-matching recognition of faces due to its robust description of local and global facial features.

A. Weighted multi-block Local Binary Pattern (WLBP)

WLBP divides face images into regions R_0, R_1, \dots, R_{m-1} (see Fig. 22 (a)) and apply Local Binary Pattern (LBP) for each region. LBP was firstly introduced by Ojala et al. [15] for the purpose of texture description and achieved high fame. The LBP operator gives each pixel a label defined by its 3×3 neighborhood. Namely the 3×3 neighborhood pixels are binarized relative to their central pixel. The decimal value of the ordered binaries is the label of the central pixel. Then the histogram of the labels can be used as a texture descriptor. In our system, we applied LBP with neighborhoods of different sizes extended by [16] and made use of the concept of uniform pattern.

The notation of $LBP_{P,R}^{u2}$ is used for the LBP operator. The subscript represents using the operator in a (P, R) neighborhood. P is the number of neighborhoods and R indicates the radius. Superscript u2 stands for using only uniform patterns and labeling all remaining patterns with a single label. A histogram of the labeled image $f_i(x, y)$ can be defined as:

$$H_i = \sum_{x,y} I\{f_i(x, y) = i\}, \quad i = 0, \dots, n-1 \quad (4)$$

where n is the number of different labels produced by the LBP operator and

$$I\{A\} = \begin{cases} 1, & A \text{ is true} \\ 0, & A \text{ is false} \end{cases} \quad (5)$$

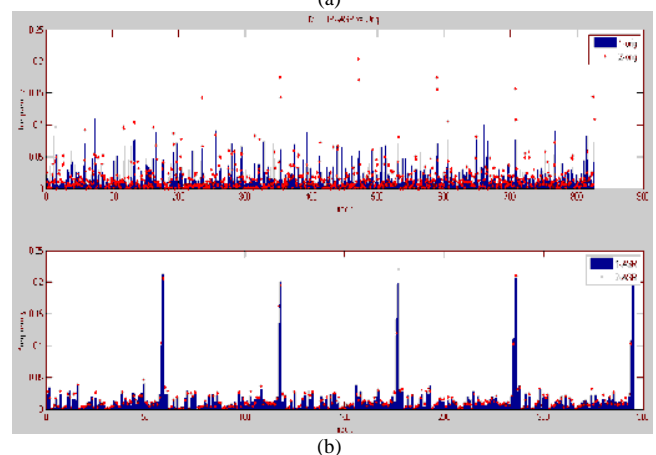


Fig. 21 (a) original face images and their corresponding ASR face images; (b): multi-block LBP bins for original face images and ASR face images. ASR is more representative for human facial features

This LBP histogram contains information about the distribution of the local micro-patterns, such as edges, spots and flat areas, over the whole image, but for efficient face representation, one should retain also spatial information. For this purpose, multi-block LBP was applied. The spatially enhanced histogram can be defined as:

$$H_{i,j} = \sum_{x,y} I\{f_i(x,y) = i\} I\{(x,y) \in R_j\}, i=0,\dots,n-1, j=0,\dots,m-1 \quad (6)$$

In this histogram, we effectively have a description of the face on three different levels of locality: the labels for the histogram contain information about the patterns on a pixel-level, the labels are summed over a small region to produce information on a regional level and the regional histograms are concatenated to build a global description. Fig. 21 shows comparison between bins of multi-clock LBP used for original face images and ASR face images.

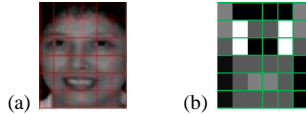


Fig. 22 (a) A sample face image divided into 6x6 windows. (b): The weights set for distance measure. Black squares indicate weight 0.0, dark grey 1.0, light grey 2.0 and white 4.0

Later weights for different parts of the face using the previously dividing blocks are set, which was proposed by [17]. The weights were selected in the paper without utilizing an actual optimization procedure and thus they are probably not optimal. In our system, according to the previous size normalization, we set the LBP blocks and face region related weights as Fig. 22 (b).

B. Distance Measures

After we represent each face's features in the form of LBP histogram, we need to use distance measures to figure out the dissimilarity between faces. Here we apply three main distance measures: 1. Euclidean distance; 2. Histogram intersection; 3. Chi square statistic (χ^2).

All of these measures can be extended to the spatially enhanced histogram (multi-block LBP) by simply summing over i and j . When applied to WLBP where a weight is set for each region based on the importance of the information it contains, the weighted χ^2 statistic becomes, for example:

$$\chi_w^2(X, Y) = \sum_{i,j} w_j \frac{(X_{i,j} - Y_{i,j})^2}{X_{i,j} + Y_{i,j}} \quad (7)$$

where w_j is the weight for region j .

C. Recognition Evaluation Principle

Suppose that we are given two color photographs as the inputs of our system as shown in Fig. 23. Also we assume that we gain five face images from the first photo and three face images from the second one after the detection and normalization. There is a label for each face image indicating which number it is and which photo it belongs to. For example, number 14 means the 4th face of the 1st photograph.



Fig. 23 The 2nd row are ordered example face images from the given two photographs in the 1st row; the number ij at the bottom of the 2nd images means the j^{th} face of the i^{th} photograph

Our proposed evaluation principle can be briefly summarized by the next two equations and illustrated in Fig. 24:

$$\min(d) = \text{Matched distance} \quad (8)$$

$$\text{Self-distance (sd)} < \text{Inter-distance (id)} \quad (9)$$

If the recognition results conform to the above equations, we say our system perform well. When the face recognition results are given, we have distances between the five face images from the first photograph and the three face images from the second photograph; each of the five face images has three distances. To begin with, we test (8). For each of the five face images, the matched distance means the distances between the same person pairs and if the matched distance is the minimum one, then the pair-matching recognition for the current face is correct otherwise incorrect. Now consider about (9). When the previous recognition is correct, the self-distance is the minimum distance and otherwise the current face image should not be passed onto the second comparison. The inter-distance is the distance of the face image having no matched face. When all inter-distances are larger than self-distances, the results are satisfactory and useful otherwise misleading. In an ideal case, further investigation may make use of thresholding method to exclude faces having no matched face.

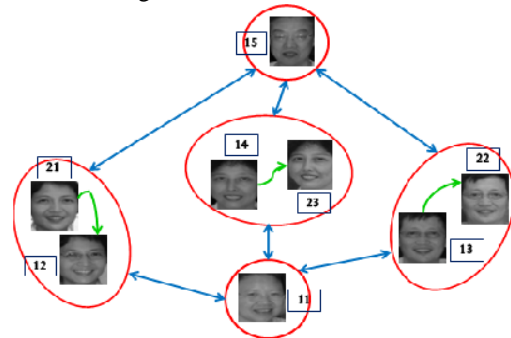


Fig. 24 Illustration of our recognition evaluation Green arrows indicate self-distances and the blue ones indicate inter-distances

V. EXPERIMENTS

In this section, we evaluate the face detection performance and the recognition performance based on our proposed evaluation principle. In our research we created a pool of human faces in form of photographs: 10 photographs with extreme illumination problems containing 64 human faces, 20 normal single photographs containing 191 faces and 15 pairs of normal photographs containing 98 faces. Each photograph of the 15 pairs contains more than 3 faces to facilitate the recognition test.

A. Face Detection

To assess the face detection, we used all of the photographs. But the detection rate will be heavily changeable if the number of photographs under extreme illumination varies. So in our experiments, we compare the performance of the method using only Haar-like face detection with the method using Haar and RHT based on the 10 extremely illuminated photographs (64 faces) and do another comparison between Haar and Haar with

skin color segmentation based on the 20 normal single photographs and 15 pairs of normal photographs (289 faces). See Fig. 25 and Fig. 26 for sample results. From Table I and Table II, we can notice that when applied with the skin color segmentation, the false detection of Haar was considerably eliminated and with RHT, the missed detection problem could be greatly rectified.

TABLE I
 DETECTION RATE FOR NORMAL PHOTOGRAPHS

Method	Detection rate (%)	
	Missed detection	False detection
Haar	9.00	27.34
Haar+skin color segmentation	13.84	6.57

TABLE II
 DETECTION RATE FOR ILLUMINATION-ORIENTED PHOTOGRAPHS

Method	Detection rate (%)	
	Missed detection	False detection
Haar	45.31	23.44
Haar+RHST	17.19	14.06



Fig. 25 Some results showing the performance of Haar-like face detection versus Haar with skin color segmentation based on photographs with variously situated faces



Fig. 26 Comparisons between Haar (1st row), HST (2nd row) and RHST (3rd row) for face detection

B. Face Recognition

In this part, the 15 pairs of normal photographs were used for testing. We assessed the pair-matching recognition performance strictly based on the two evaluation equations ((8) and (9)).



Fig. 27 A pair of original color photographs

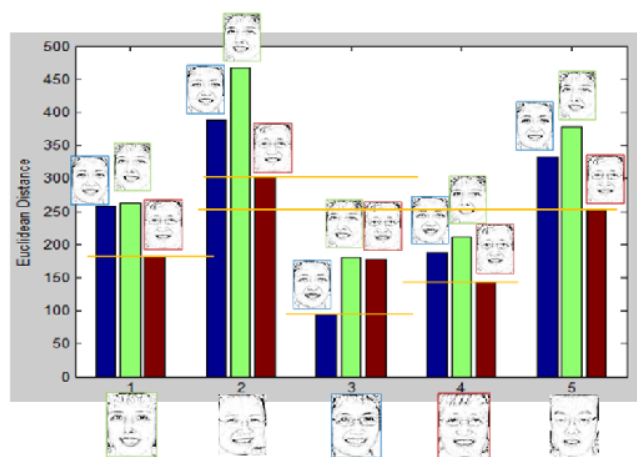


Fig. 28 Pair-matching recognition result using PCA with Euclidean distance measure

First we tested Principle Component Analysis (PCA) [18] applied to our system. During this experiment, we gain facial features for each face image via calculating 20 eigenfaces from the ORL database and use Euclidean distance measure to tackle the facial features. Fig. 28 shows the result based on the pair of photographs in Fig. 27. The horizontal axis represents the five face images from the first photograph and the perpendicular axis represents the distances these five face images and the three face images from the second photograph. According to the recognition evaluation principle, the third and the fourth are correctly recognized but the first one is incorrect. So it does not match (8). For the second and the fifth face images, there are no

corresponding face images in the other photograph but their smallest distances are larger than all matched distances, which conforms to (9).

In the same evaluation way, we tested PCA, multi-block LBP and WLBP with 3 distance measures on 15 pairs of color photographs. Table III gives the recognition results, from which we notice that WLBP applied with Chi square statistic distance measure can achieve relatively better recognition in terms of conformity to our proposed evaluation equations.

TABLE III
 RECOGNITION RATE FOR 15 PHOTOGRAPH PAIRS

Distance measure		Recognition rate (%)		
		PCA	multi-block LBP	WLBP
Euclidean distance	(8)	0.00	20.00	20.00
	(9)	33.33	33.33	46.67
Histogram intersection	(8)	13.33	66.67	66.67
	(9)	33.33	60.00	80.00
Chi square statistic (χ^2)	(8)	13.33	66.67	86.67
	(9)	33.33	80.00	80.00

VI. CONCLUSION

This paper has constructed a novel face recognition system as a pair-matching problem based on natural color photographs. The method of combination of Haar-like feature detection, skin segmentation and region-based histogram stretching and truncation (RHST) is proposed to achieve fast and more accurate performance than using only Haar-like face detection. Geometric and illumination normalization are implemented then, and they are effective in gaining upright and balancedly illuminated face images. The HST method is relatively qualified in balancing the overall extreme and uneven illumination and is used in the face detection step; ASR shows better illumination removing ability and is used for illumination normalization. In addition, the side-face normalization is specially proposed, which seems effective and valuable for further investigation. For the face recognition part, based on the proposed evaluation principle, experimental results show us that WLBP applied with Chi square statistic distance measure can achieve relatively better recognition compared with PCA and simple multi-block LBP.

Our research, up to now, has some inadequacy such as that the proposed face detection method is still unstable which may result in false or missed detection and that some verification experiments are limited and not persuasive enough. So in the future, we may continue to improve our system and focus on the coherency and automaticity, and also deal with particular parts of the system such as side-face normalization or more applications of efficient face recognition algorithms.

REFERENCES

[1] M. H. Yang, and D. J. Kriegman, Detecting Faces in Images: A Survey, *IEEE Transactions on Pattern Analysis and Machine Intelligence*, Vol. 24, No. 1, Jan. 2002, pp. 34 - 58.E.
 [2] Hjelmas, and B. K. Low, Face Detection: A Survey, *Computer Vision and Image Understanding*, Vol. 83, No. 3, Sept. 2001, pp. 236-274.
 [3] http://en.wikipedia.org/wiki/Facial_recognition_system.

[4] Paul Viola, and M. J. Jones, Rapid Object Detection using a Boosted Cascade of Simple Features, *IEEE Conference on Computer Vision and Pattern Recognition*, 2001.
 [5] Crow, F, Summed-area tables for texture mapping, *Proceedings of SIGGRAPH*, 1984, 18(3):207-212.
 [6] Freund, Y. and Schapire, R.E. A decision-theoretic generalization of on-line learning and an application to boosting. In *Computational Learning Theory: Eurocolt 95*, Springer-Verlag, 1995, pp. 23-37.
 [7] http://en.wikipedia.org/wiki/File:Prm_VJ_fig4_cascadeWithAlpha.png.
 [8] <http://www-cs-students.stanford.edu/~robles/ee368/skincolor.htmlNusirwan>.
 [9] A. Rahman, Kit C. Wei and John See. RGB-H-CbCr Skin Colour Model for Human Face Detection. In *Proceedings of The MMU International Symposium on Information & Communications Technologies*. 2006.
 [10] Otsu N. A threshold selection method from gray-level histogram, *IEEE Trans. Syst. Man Cybern.* 1979, 9(1):62-66.
 [11] K.T. Talele and Sunil Kadam. Face Detection and Geometric Normalization. In *IEEE Region 10 Conference*, Jan. 2009, pp. 1-6.
 [12] Štruc, V. and Pavešić, N.: *Illumination Invariant Face Recognition by Non-Local Smoothing*, In: *Proceedings of the international Cost 2101 & 2102 conference BioID_MultiComm 2009*, pp. 1-8.
 [13] Y. K. Park, S. L. Park, and J. K. Kim. Retinex method based on adaptive smoothing for illumination invariant face recognition. *Sig. Proces.*, 2008, Vol. 88, No. 8, pp. 1929-1945.
 [14] Georghiades, A.S. and Belhumeur, P.N. and Kriegman, D.J. From Few to Many: Illumination Cone Models for Face Recognition under Variable Lighting and Pose. *IEEE Transactions on Pattern Analysis and Machine Intelligence*, Vol. 23, No. 6, 2001, pp. 643-660.
 [15] Ojala, T., Pietikinen, M., Harwood, D. A comparative study of texture measures with classification based on feature distributions. *Pattern Recognition*, vol. 29, 1996, pp.51-59.
 [16] Ojala, T., Pietikinen, M., Mäenpää, T. Multiresolution gray-scale and rotation invariant texture classification with local binary patterns. *IEEE Transactions on Pattern Analysis and Machine Intelligence*, vol.24, 2002, pp. 971-987.
 [17] Pietikinen, M., Ahonen, T., Hadid, A. Face recognition with local binary patterns. In: Pajdla, T., Matas, J(G.) (eds.) *ECCV 2004*. LNCS, vol. 3021, pp. 469-481. Springer, Heidelberg.
 [18] M. Turk and A. Pentland, "Eigenfaces For Recognition," *Journal Of Cognitive Neuroscience*, Vol.3, pp.71-86, 1991.